Rotating Stall in Axial Compressors[1])

By WILLIAM R. SEARS, Ithaca, New York[2])

Introduction

Experiments carried out in axial-flow compressors by several investigators [1], [2], [3][3]) have disclosed that violently asymmetrical flow patterns occur in such machines when their flow rate is so restricted as to cause blade stalling. Typically, certain portions of the annulus of blades appear to be stalled while others remain unstalled; the stalled portions exhibit reduced airflow and the roughness of flow characteristic of stalling. But what seems most important is the fact that these patterns of stalled and unstalled flow do not remain fixed to either the stator or the rotor blades, but rotate steadily in the direction of rotor rotation at a lower speed than that of the rotor blades. The result is that both rotor and stator blades are subjected to violent periodic aerodynamic loads, since they find themselves alternatively in stalled and unstalled flow.

The experiments mentioned above [1], [2], [3] were carried out with the aid of hot-wire anemometers. One wire attached to a stator row is sufficient to disclose that a periodic flow occurs; several wires, spaced circumferentially in a stator row provide, in addition, information concerning the rate of rotation of the asymmetrical flow pattern. Patterns having one stalled region have been observed, and also patterns having several, equally spaced regions. The regions of stalled flow may extend across the annulus from blade root to tip (Figure 1), or they may lie near the blade roots (Figure 2) or near the blade tips.

There are, in fact, interesting differences between the results obtained by the various experimenters. What is common to them is principally the fact already stated above: that stalling of axial-flow compressors is accompanied by the appearance of steadily-rotating periodic stall patterns. This conclusion has been so generally reached that it may even be surmised that all axial-flow compressors and pumps behave in this way. If this is correct, it may provide an explanation of numerous fatigue failures of blades, which have previously been blamed on flutter or stall flutter, or on other causes.

It should also be made clear that this phenomenon is not the familiar one known as 'surge', which involves periodic variation of the rate of flow through

[1]) This research was partially supported by the United States Air-Force under Contract No. AF 33 (038)-21406, monitored by the Office of Scientific Research, Air Research and Development Command.

[2]) Graduate School of Aeronautical Engineering, Cornell University.

[3]) Numbers in brackets refer to References, page 454.

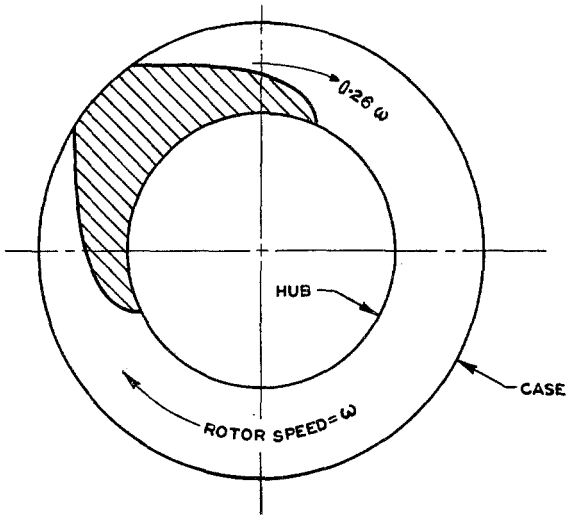

Figure 1
Depiction of rotating-stall pattern [2]. Three-stage compressor.

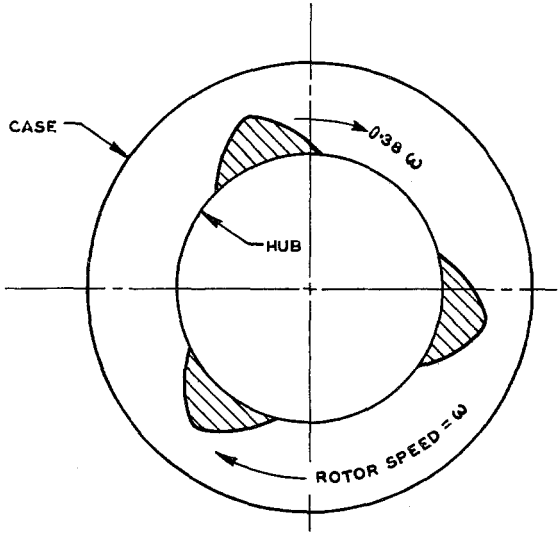

Figure 2
Depiction of rotating-stall pattern [2]. Three-stage compressor. Slightly higher flow than for Figure 1.

the machine. This distinction has already been pointed out clearly [1], [2], but still seems to require emphasis. The phenomenon of rotating stall is basically one involving steady flow through the machine; only its distribution around the annulus is nonuniform. The flow, in fact, becomes a truly steady flow when viewed from a coordinate system rotating with the stall pattern—a fact that will be exploited farther below. To be sure, the two phenomena, rotating stall and surge, may occur together, and it appears that the non-uniqueness of the rotating-stall type of flow for any certain flow rate may be one of the chief sources of the instability that we call surge [2].

The present paper is a review of several attempts to explain the phenomenon of rotating stall on a theoretical basis. As will be seen, the attempts have not been entirely successful to date, especially because they concern a type of flow – unsteady, stalled flow – about which there is insufficient knowledge. On the other hand, they are not completely unsuccessful, since they show, at least qualitatively, that flow patterns of the rotating-stall type may occur in axisymmetrical rigid blade rows with steady, uniform inflow to the machine. This conclusion is of some importance. It seems clear that stall flutter, for example, could produce periodic flow patterns that would rotate around the blade annulus if the flutter frequency were not the same as, or a multiple of, the rotational frequency. But the occurrence of stall flutter must depend intimately on the elastic properties of the blades. Thus it is important to know whether a similar phenomenon can occur purely aerodynamically, in a row of rigid blades.

Notations

A	constant in equation (35);
b	V/U (Figure 3);
B	constant in equation (35);
c_l	lift coefficient of blade; $c_l[\alpha]$ denotes the lift coefficient as function of α, while $c_l(y)$ represents the same quantity as function of y; i.e., $c_l[\alpha(y)] \equiv c_l(y)$;
C	constant in equation (35);
C_1, C_2	constants in equations (8) to (12);
h	$h(y) = \Delta H/\varrho\, U^2$;
h_n	Fourier coefficient of $h(y)$;
H	$H(x, y)$ = total pressure;
ΔH	$\Delta H(y)$ = increase of H across blade row at y;
k	circumferential speed of blades relative to flow pattern, divided by axial flow speed U; positive in negative y direction;
K_1, K_2	constants in equations (38) and (42);
l	circumference of blade wheel;

m (local) slope of the curve $c_l[\alpha]$ (per radian);
M (local) slope of h against β_i in channel relations;
n coordinate normal to undisturbed stream direction [Figure 3 and equation (3)];
n summation index of Fourier series;
p $p(x, y)$ = static pressure;
Δp $\Delta p(y)$ = static pressure rise across blade row;
$\Re$ real part;
t time;
u $u(x, y)$ = perturbation axial velocity component;
u_n Fourier coefficient of $u_0(y)$;
$u_0(y)$ $u(0, y)$;
U undisturbed axial velocity component;
v $v(x, y)$ = perturbation circumferential velocity component;
$v_-(y)$ $v(-0, y)$;
$v_+(y)$ $v(+0, y)$;
V bU undisturbed circumferential velocity component;
x axial coordinate (Figure 3);
y circumferential coordinate (Figure 3);
α $\alpha(y) = (\beta_i + \beta_0)/2$; mean angle of attack;
α_n Fourier coefficient of $\alpha(y)$;
β_i $\beta_i(y)$ inlet angle relative to blade (Figure 4);
β_i mean (unperturbed) value of β_i;
β_o $\beta_o(y)$ outlet angle relative to blade (Figure 4);
β_n Fourier coefficient of $\beta_i(y)$;
δ angle of phase lag of h behind β_i;
Δ angle of phase lag of c_l behind α;
η variable of integration;
$\varkappa$ flow coefficient [equation (36)];
ϱ density of fluid;
σ solidity of blade row (= chord/gap);
ψ $\psi(x, y)$ = stream function;
Ω $\Omega(x, y)$ = vorticity.

Subscripts, superscripts, etc.

$( )_{-\infty}$ value at $x = -\infty$;
$( )_{\infty}$ value at $x = +\infty$;
$( )_c$ value given by the uniform-turning solution;
$( )^{(2)}$ rotational part of $(\tilde{\ })$;
$( )^{(1)}$ irrotational part of $(\tilde{\ })$;
$(\tilde{\ })$ variable part of $( )$, defined by $( ) = ( )_c + (\tilde{\ })$.

Flow Through a Blade Row

All of the theoretical investigations of rotating stall, to date, are based on four simplifying assumptions; viz.,

(1) The compressor is replaced by a single blade row.

(2) Assuming that the blade length, i.e., the width of the blade annulus, is small compared to the mean radius, the blade row is replaced by a two-dimensional cascade of blades.

(3) The flow is supposed to consist of a small perturbation of a uniform stream

(4) Viscosity and compressibility of the fluid are neglected.

In all but one study [5], the further approximation has been made that:

(5) The blade row consists of infinitely many blades; i.e., the row is replaced by a discontinuity surface at which energy, due to rotation of the blades, is introduced to the flow.

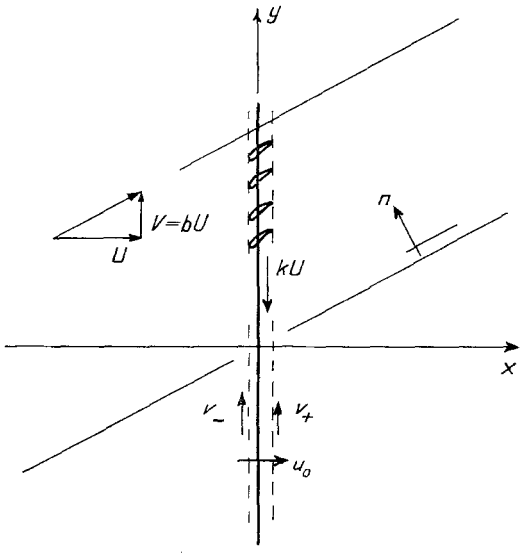

Figure 3
Diagram showing coordinate system and notation.

In the lone exception, which is an unpublished investigation [5], a row of discrete blades was first treated. To render the results practically useful, however, the same approximation of vanishing chords and blade spacing was later introduced, so that the work finally fell into the same category.

The two-dimensional incompressible-flow problem resulting from these assumptions is sketched in Figure 3. The discontinuity surface lies along the

y-axis. It will now be assumed that the flow pattern is a steadily rotating one, as has been described above, and the coordinate system will be defined to be fixed relative to this moving pattern. The flow is thereby rendered steady, with a consequent simplification of the analysis. For example, BERNOULLI'S equation can now be used to describe the flow either upstream or downstream of the discontinuity sheet. It should be recognized that the analysis applies equally well to a stator or a rotor row, since there is no distinction between these from the point of view of the coordinate system employed.

Other notation to be employed in the analysis is indicated in Figure 3 and in Notations, page 431. So far, the problem is formulated exactly as in Reference [4] except that the swirl angle relative to the moving coordinate system, $\tan^{-1} b$, is not assumed to be small. The appropriate, linearized Bernoulli equation is, for $x < 0$,

$$p + \varrho U u + \varrho V v = p_{-\infty}, \tag{1}$$

where u and v are the perturbation velocity components and $p_{-\infty}$ is the pressure far upstream where conditions are uniform.

Let the total-pressure rise through the blade row be $\Delta H(y)$. Simply to provide a dimensionless representation of this quantity, let $\Delta H(y)/(\varrho U^2)$ be denoted by $h(y)$. The Bernoulli equation for the downstream region is then the statement that $p + \varrho U u + \varrho V v$ is constant and equal to $p_{-\infty} + \Delta H$ along any streamline. Within the scope of a small-perturbation theory, however, this statement can be revised as if the streamlines lay in the direction of the undisturbed flow. Thus, for $x > 0$,

$$p + \varrho U u + \varrho V v = p_{-\infty} + \varrho U^2 h(y - b x) = H(x, y). \tag{2}$$

In Reference [4] the vorticity in the flow downstream of the actuator was calculated by consideration of the shedding of vortices by the blades as they pass through a variable flow pattern. Actually, this resort to airfoil theory is unnecessary, since for steady flow there is a simple relation between the vorticity Ω and the gradient of the total pressure H. This relation is, for the present application [10],

$$\frac{\partial H}{\partial n} = -\varrho \sqrt{U^2 + V^2}\,\Omega(x, y), \tag{3}$$

where $\partial H/\partial n$ denotes the derivative of H in the direction normal to the undisturbed streamlines; viz.,

$$\frac{\partial H}{\partial n} = \frac{\partial H}{\partial y} \cdot \frac{U}{\sqrt{U^2 + V^2}} - \frac{\partial H}{\partial x} \cdot \frac{V}{\sqrt{U^2 + V^2}} = \varrho U h'(y - b x) \sqrt{U^2 + V^2}.$$

Therefore the vorticity is

$$\Omega(x, y) = - U h' (y - b x) . \tag{4}$$

The boundary conditions far upstream are the vanishing of all perturbation quantities. The boundary condition far downstream is the condition of uniform pressure and parallel flow. The condition of parallel flow is

$$\frac{V + v}{U + u} \approx \frac{V}{U} \left(1 + \frac{v}{V} - \frac{u}{U}\right) = \text{constant} \tag{5}$$

or

$$\frac{v}{V} - \frac{u}{U} = \text{constant} . \tag{6}$$

It should be noticed that the direction of this parallel flow is not specified; it differs, in fact, from the direction of incoming flow. Nevertheless, this condition is sufficient to establish conditions at $x = \infty$, except for constant terms not required in the analysis, for equation (6) leads to

$$\Omega = \frac{\partial v}{\partial x} - \frac{\partial u}{\partial y} = b \frac{\partial u}{\partial x} - \frac{\partial u}{\partial y} \tag{7}$$

at $x = \infty$.

With Ω given by equation (4), it is easily verified that the solution of this differential equation for u is

$$u_\infty = U (1 + b^2)^{-1} h (y - b x) + C_1 , \tag{8}$$

and therefore

$$v_\infty = U b (1 + b^2)^{-1} h (y - b x) + C_2 . \tag{9}$$

These values, u_∞ and v_∞, are the asymptotic values of u and v far downstream, while C_1 and C_2 are constants involved in the uniform-turning part of the solution, which is discussed below. It is easily verified, by substitution in equation (2), that these yield a constant value for p_∞.

The Uniform-Turning Solution

Having established the flow conditions far upstream and far downstream, it is now possible to identify a solution consisting entirely of constants, which represents uniform turning of the flow through the blade row. Let these values be denoted by the subscript c. They are

For $x < 0$:

$$u_c = 0 = v_c\,, \quad p_c = p_{-\infty}\,.$$

For $x > 0$:

$$u_c = 0 = \frac{1}{1+b^2}\,U\,h_c + C_1\,, \quad v_c = \frac{b}{1+b^2}\,U\,h_c + C_2\,,$$

$$p_c = p_{-\infty} - \varrho\,V\,C_2 + \varrho\,\frac{1}{1+b^2}\,U^2 h_c = p_\infty$$

or

$$\varrho\,U^2 h_c = p_\infty - p_{-\infty} + \varrho\,V\,v_c$$

and

$$\Omega_c = 0\,. \tag{10}$$

The Boundary-Value Problem

The uniform-turning solution is a trivial one so far as the phenomenon of rotating stall is concerned. To proceed to more interesting solutions it is necessary to work out the relations that exist between the flow variables both upstream and downstream of the blade row. These are, of course, different in the two regions because the flow upstream is irrotational while that downstream is rotational. The two regions are related at the blade row ($x = 0$) by the continuity of the axial flow component and by the characteristics of the blades themselves, which will be discussed later. Let the velocity components just upstream of the blade row be called $u_0(y)$ and $v_-(y)$. Then the value of u just downstream of the row must also be $u_0(y)$, while the tangential component will, in general, jump to a different value $v_+(y)$.

In terms of the familiar plane stream function $\psi(x, y)$ whose derivatives are $\psi_y = u$ and $\psi_x = -v$, the boundary-value problems of the upstream and downstream regions are, for $x < 0$:

$$\nabla^2 \psi = 0\,, \quad u(-\infty, y) = 0 = v(-\infty, y)\,,$$

$$p(-\infty, y) = p_{-\infty} = \text{constant}\,, \quad u(-0, y) = u_0(y)\,, \quad v(-0, y) = v_-(y)\,. \tag{11}$$

For $x > 0$:

$$\nabla^2 \psi = -\Omega = U\,h'\,(y - b\,x)\,,$$

$$u(\infty, y) = \frac{1}{1+b^2}\,U\,h(y - b\,x) + C_1\,,$$

$$v(\infty, y) = \frac{b}{1+b^2}\,U\,h\,(y - b\,x) + C_2\,,$$

$$p(\infty, y) = p_{-\infty} - \varrho\,U\,C_1 - \varrho\,V\,C_2\,,$$

$$u(+0, y) = u_0(y)\,, \quad v(+0, y) = v_+(y)\,. \tag{12}$$

For convenience, let all these quantities be considered as made up of the constant-turning parts, equations (10), and variable parts denoted by the sign $(\tilde{\ })$; i.e., $\psi = \psi_c + \tilde{\psi}$, etc. Then, since the former consist of undisturbed flow upstream, equations (11) are the equations for $\tilde{\psi}$, $\tilde{u}$, $\tilde{v}$, and $\tilde{p}$, except for the boundary condition $\tilde{p}(-\infty, y) = 0$. Equations (12), on the other hand, are replaced, for $x > 0$, by:

$$
\left.
\begin{aligned}
&\nabla^2 \tilde{\psi} = -\tilde{\Omega} = -\Omega = U \tilde{h}'(y - b\,x)\,, \\
&u = \tilde{u}; \quad u(\infty, y) = \frac{1}{1 + b^2}\, U h(y - b\,x) + C_1 \\
&\qquad \tilde{u}(\infty, y) = \frac{1}{1 + b^2}\, U \tilde{h}(y - b\,x)\,, \\
&\qquad \tilde{v}(\infty, y) = \frac{b}{1 + b^2}\, U \tilde{h}(y - b\,x)\,, \\
&\qquad \tilde{p}(\infty, y) = 0\,, \quad \tilde{u}(+0, y) = u_0(y)\,, \\
&\qquad \tilde{v}(+0, y) = v_+(y) - v_c \equiv \tilde{v}_+(y)\,.
\end{aligned}
\right\} \tag{13}
$$

The solution of equations (11) can be written down immediately in the form of definite-integral relations between $u_0(y)$ and $v_-(y)$. One can consider these as resulting from a distribution of sinks along the y-axis, of strength $2\,u_0(y)$ or from a distribution of vortices of strength $2\,v_-(y)$. The results, which are strictly equivalent, are

$$
u_0(y) = \frac{1}{\pi} \int_{-\infty}^{\infty} \frac{v_-(\eta)\, d\eta}{y - \eta} \quad \text{and} \quad v_-(y) = -\frac{1}{\pi} \int_{-\infty}^{\infty} \frac{u_0(\eta)\, d\eta}{y - \eta} \tag{14}
$$

where the integrals are Cauchy principal values.

The solution of equations (13) can be constructed by the same technique after a particular solution of the Poisson equation is subtracted out. A suitable rotational flow for this purpose is the parallel shear flow far downstream, given by $\tilde{u}(\infty, y)$, $\tilde{v}(\infty, y)$ in equations (13). In other words, let

$$
\tilde{u} = u^{(1)} + u^{(2)} \quad \text{with} \quad u^{(2)} = \frac{1}{1 + b^2}\, U \tilde{h}(y - b\,x) \tag{15}
$$

and

$$
\tilde{v} = v^{(1)} + v^{(2)} \quad \text{with} \quad v^{(2)} = \frac{b}{1 + b^2}\, U \tilde{h}(y - b\,x)\,. \tag{16}
$$

Then, with $\tilde{\psi} = \psi^{(1)} + \psi^{(2)}$, one has for the downstream region,

$$\left.\begin{aligned} \nabla^2 \psi^{(1)} = 0\,, \quad & u^{(1)}(\infty, y) = 0 = v^{(1)}(\infty, y)\,, \\ u^{(1)}(+0, y) = u_0(y) - u^{(2)}(0, y) &= u_0(y) - \frac{1}{1+b^2}\, U\tilde{h}(y)\,, \\ v^{(1)}(+0, y) = \tilde{v}_+(y) - v^{(2)}(0, y) &= \tilde{v}_+(y) - \frac{b}{1+b^2}\, U\tilde{h}(y)\,. \end{aligned}\right\} \tag{17}$$

The relations analogous to equations (14) are then

$$\left.\begin{aligned} u_0(y) - \frac{1}{1+b^2}\, U\tilde{h}(y) &= -\frac{1}{\pi}\int_{-\infty}^{\infty} \frac{\tilde{v}_+(\eta) - U\tilde{h}(\eta)\, b/(1+b^2)}{y-\eta}\, d\eta \\ \text{and} \qquad & \\ \tilde{v}_+(y) - \frac{b}{1+b^2}\, U\tilde{h}(y) &= \frac{1}{\pi}\int_{-\infty}^{\infty} \frac{u_0(\eta) - U\tilde{h}(\eta)/(1+b^2)}{y-\eta}\, d\eta\,. \end{aligned}\right\} \tag{18}$$

Thus, the velocity components upstream of the blade row are definitely related to one another, while those downstream are related in a way that involves the total-pressure-rise function $\tilde{h}(y)$.

All the small-perturbation analyses of the rotating-stall phenomenon are basically the same up to this point, although some of the authors have not made use of the steady-flow coordinate system, and have had to look for those special unsteady solutions that do not grow or decay as they propagate. At this point one has just two relations, equations (14) and (18), between four unknown functions,

$$u_0(y)\,, \quad v_-(y)\,, \quad \tilde{v}_+(y)\,, \quad \text{and} \quad \tilde{h}(y)\,.$$

The other two relations needed may be called the 'blade-characteristic' relations; it is in the choice of these that our ignorance of the precise nature of stalled flow becomes apparent and in which the various analyses of the phenomenon diverge from one another.

Before proceeding to discuss the various assumptions that have been made regarding blade characteristics, it may be of interest to consider briefly the physical and mathematical natures of the solutions sought. The fundamental unknown function is the pressure rise $\tilde{h}(y)$, which describes the loading of the blades. The equations derived above state the relations that exist between this loading and the induced velocities $u_0(y)$, $v_-(y)$, and $\tilde{v}_+(y)$. The blade-characteristic relation will tell how the loading is affected by variations of the velocity and flow direction at the blade row; i.e., ultimately, how $\tilde{h}(y)$ is affected by the

same induced velocity components. Thus, the problem is strictly a homogeneous one: What nonuniform blade loading function induces such velocity components as just to support itself?

There is an analogous problem in the realm of lifting-line wing theory: What spanwise circulation distribution induces such a downwash distribution as just to support itself? It is easy to show (and seems physically obvious) that for unstalled wings PRANDTL's equation admits no trivial solution to this problem. If the slope of the section lift curve is negative, however, the homogeneous Prandtl equation has infinitely many eigen-solutions, but only for eigen-values of the slope [11]. One is not surprised to find that the rotating-stall problem has analogous solutions, which will be discussed farther below.

Blade-Characteristic Relations of Airfoil Type

In References [4] and [5], the two additional relations needed to connect the upstream and downstream regions of flow were carried over from airfoil theory. It was envisaged that, even in conditions of partial stall, the most important force acting on a blade would be the lift, or more precisely, the component arising from circulation. This is the force that, in a stationary cascade, would produce a pure deflection of the flow without gain or loss of total pressure; in a moving cascade, of course, it results in a change of total pressure. Taking into account this force alone, the first blade-characteristic relation was written by equating the rise of total head to the axial force exerted by the moving blade. Since the circulation per unit length of the discontinuity sheet is $v_- - v_+$, this relation is

$$\left.\begin{aligned} \Delta H(y) &= \varrho\, k\, U\, [v_-(y) - v_+(y)] \\ \text{or} \qquad h(y) &= \frac{k\,[v_-(y) - v_+(y)]}{U}, \end{aligned}\right\} \tag{19}$$

where $k\,U$ denotes the velocity of the blades relative to the moving coordinate system.

The second relation, according to this formulation of the problem, is that connecting the blade circulation $v_- - v_+$ to the blade angle of attack α:

$$v_-(y) - v_+(y) = \frac{1}{2}\,\sigma\, U \sqrt{1 + (b + k)^2}\; c_l[\alpha]\,, \tag{20}$$

where σ denotes the solidity of the blade row and $c_l[\alpha]$ is the lift-coefficient curve of the blades, which is nonlinear, in general. According to the theory of airfoils in cascades, and neglecting unsteady-flow effects on the ground that the wave lengths of flow patterns are large compared to the blade chord (already

neglected), one should use here the mean angle of attack

$$\alpha = \frac{1}{2}(\beta_i + \beta_o).$$

It is easy to compute this angle as the sum of arc tangents and then to linearize

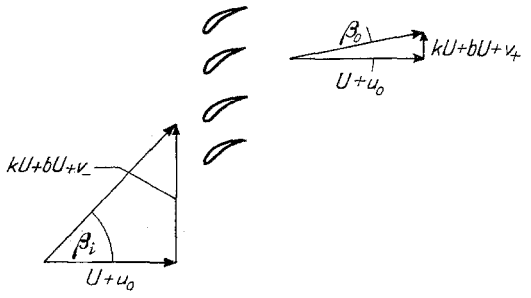

Figure 4
Diagram showing inlet and outlet angles, β_i and β_o.

the result in accordance with the small-perturbation hypothesis. The result gives α in the form $\alpha_c + \tilde{\alpha}$ where α_c corresponds to the uniform turning solution discussed above. The variable part, $\tilde{\alpha}$, is found to be

$$\tilde{\alpha} = \frac{1/2\,(v_- + \tilde{v}_+) - (k+b)\,u_0}{U[1+(b+k)^2]}. \tag{21}$$

The second relation may now be written in terms of perturbation quantities:

$$v_-(y) - \tilde{v}_+(y) = \frac{1}{2}\,\sigma\,U\sqrt{1+(b+k)^2}\,\tilde{c}_l[\tilde{\alpha}], \tag{22}$$

where $\tilde{c}_l[\tilde{\alpha}]$ is, of course, the lift-coefficient function measured from the constant-turning point $c_{l_c} \equiv c_l[\alpha_c]$ (Figure 5).

Linearized lift-coefficient curve. Phase lag

It seems most consistent with the small-perturbation assumption to linearize the curve at this point, i.e., to replace the curve $\tilde{c}_l[\tilde{\alpha}]$ by its tangent, and to write

$$\tilde{c}_l[\tilde{\alpha}(y)] = m\,\tilde{\alpha}(y) \quad (m = \text{constant}). \tag{23}$$

This is the type of approximation made in Reference [4] and included in a more general framework in Reference [7]. In both cases, moreover, the phenomenon of time lag was also included in an approximate way. It is well known

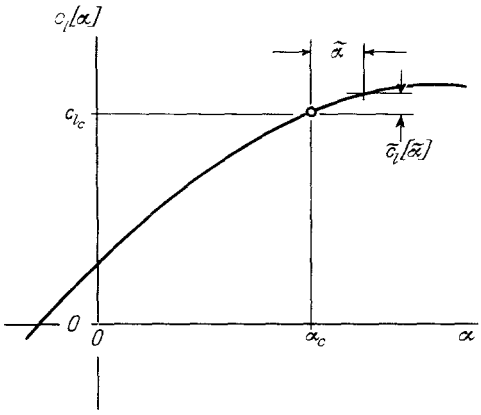

Figure 5
Diagram defining lift-coefficient functions $c_l[\alpha]$ and $\tilde{c}_l[\tilde{\alpha}]$.

that the circulation about an airfoil lags behind its incidence by an interval which is greater at large angles of attack than at small. This time lag is due primarily to the time required for the viscous processes of separation and vortex shedding after a change of incidence, and may be considerably larger than the subsequent time lag in the build-up of circulation according to the theory of airfoils in unsteady motion. It has been studied by MENDELSON [6], who concluded that, approximately, the *phase* lag for any airfoil in oscillatory motion depends on the mean incidence and not on the frequency of oscillation.

This interesting result presumably cannot apply to all frequencies, but was proposed as an approximation for the range of frequencies involved in many cases of stall flutter. In the present application it states that, if the angle-of-attack perturbation is sinusoidal:

$$\tilde{\alpha}(y) = \mathcal{R}\left\{\alpha_n e^{2\pi i n y/l}\right\}, \tag{24}$$

where α_n, n, and l are constants, l being the circumference of the blade wheel, then the corresponding lift coefficient is

$$\tilde{c}_l(y) = m\,\mathcal{R}\left\{\alpha_n e^{i\left[2\pi n (y/l) + \Delta\right]}\right\}, \tag{25}$$

where the phase-lag angle Δ depends upon α_c but not upon α_n or n. (Here the symbol $\mathcal{R}$ has been used to denote the real part of a complex quantity. In what follows, this symbol will be omitted, and real parts always implied.)

To utilize these relations, suppose $\tilde{h}(y)$ to be expanded in a Fourier series. It must have a period equal to l. Thus,

$$\tilde{h}(y) = \sum_{n=1}^{\infty} h_n e^{2\pi i n y/l}. \tag{26}$$

The corresponding induced angle of attack $\tilde{\alpha}(y)$ then has the form

$$\tilde{\alpha}(y) = \sum_{n=1}^{\infty} \alpha_n e^{2\pi i n y/l}, \tag{27}$$

and equation (25) states that

$$\tilde{c}_l(y) = m \sum_{n=1}^{\infty} \alpha_n e^{i[2\pi n (y/l) + \Delta]}. \tag{28}$$

But the Fourier coefficients α_n are easily found by means of the equations derived above, viz., equation (21) for $\tilde{\alpha}$ together with equations (14) and (18). In particular, one finds that

$$\left.\begin{aligned} v_-(y) + v_+(y) &= \frac{b}{1+b^2}\, U \tilde{h}(y) - \frac{1}{\pi} \cdot \frac{U}{1+b^2} \int_{-\infty}^{\infty} \frac{\tilde{h}(\eta)\, d\eta}{y-\eta} \\ &= U \frac{b+i}{1+b^2} \sum_{n=1}^{\infty} h_n e^{2\pi i n y/l} \end{aligned}\right\} \tag{29}$$

and

$$\left.\begin{aligned} 2 u_0(y) &= \frac{1}{\pi} \int_{-\infty}^{\infty} \frac{v_-(\eta) - \tilde{v}_+(\eta)}{y-\eta}\, d\eta + \frac{U}{1+b^2}\, \tilde{h}(y) + \frac{1}{\pi} \cdot \frac{U b}{1+b^2} \int_{-\infty}^{\infty} \frac{\tilde{h}(\eta)\, d\eta}{y-\eta} \\ &= \frac{U}{k} \cdot \frac{1}{\pi} \int_{-\infty}^{\infty} \frac{\tilde{h}(\eta)\, d\eta}{y-\eta} + U \frac{1-b\,i}{1+b^2} \sum_{n=1}^{\infty} h_n e^{2\pi i n y/l} \\ &= U \left\{ -\frac{i}{k} + \frac{1-b\,i}{1+b^2} \right\} \sum_{n=1}^{\infty} h_n e^{2\pi i n y/l}, \end{aligned}\right\} \tag{30}$$

so that

$$\tilde{\alpha}(y) = \frac{-1/2}{1+(b+k)^2} \left\{ \frac{k}{1+b^2} - i \left[\frac{b}{k} + 2 + \frac{k\,b}{1+b^2} \right] \right\} \sum_{n=1}^{\infty} h_n e^{2\pi i n y/l}. \tag{31}$$

The coefficient of $e^{2\pi i n y/l}$ in this expression is the Fourier coefficient α_n of equation (27); thus $\tilde{c}_l(y)$ follows from equation (28), and equation (22) becomes

$$\sum_{n=1}^{\infty} h_n e^{2\pi i n y/l} = \frac{1}{2}\, m \sigma k \sqrt{1+(b+k)^2} \sum_{n=1}^{\infty} \alpha_n e^{i[2\pi n (y/l) + \Delta]}. \tag{32}$$

This is the complete equation of the problem, according to the present approximations. It is the statement that the loading $\tilde{h}(y)$ is supported by its own induced velocities. It is, as was mentioned above, a homogeneous equation, and can be satisfied in a nontrivial way only when the successive Fourier

constants on the right- and left-hand sides are equal; i.e.,

$$h_n = \frac{1}{2} m \sigma k \sqrt{1 + (b + k)^2}\, \alpha_n e^{i\Delta} \tag{33}$$

with α_n taken from equation (31). This requires both

$$\left.\begin{aligned} &\frac{k^2 b}{1 + b^2} + 2k + b = \frac{k^2}{1 + b^2} \tan \Delta \\ \text{and} \qquad &-\frac{m\sigma}{4} = \frac{1 + b^2}{k^2} \sqrt{1 + (b + k)^2}\, \cos \Delta. \end{aligned}\right\} \tag{34}$$

The simultaneous solutions of these two equations, for various assumed values of Δ, are plotted in Figure 6. The most convenient independent variable

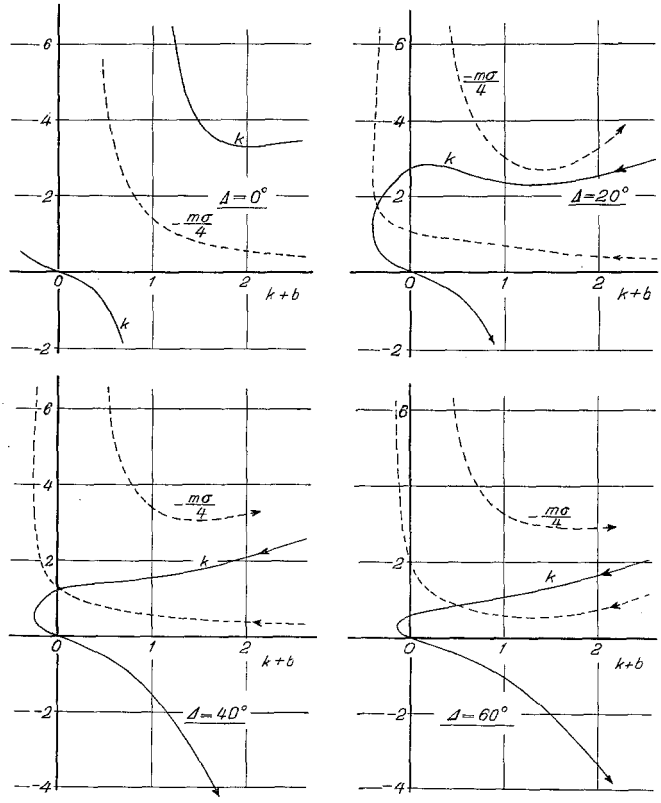

Figure 6

Rotating-stall solutions based on blade-characteristic relations of airfoil type. The abscissa, $k + b$, is the tangent of the mean inlet angle β_i. Where double-valued functions occur, corresponding values of k and $-m\sigma/4$ are to be read from branches showing arrowheads in the same direction.

is $k + b$, which is the tangent of the mean (undisturbed) angle of inflow relative to the moving blade; i.e., the mean value of β_i in Figure 4, say β_i. This is a parameter of clear geometrical meaning, easily estimated from design data for any given blade row in a turbo-machine at any known flow rate. Equations (34) state that, for any given value of this parameter and for any known value of Δ, rotating stall can occur only for two special values of $m\,\sigma$—both negative—and that the stall pattern must rotate at certain corresponding speeds $k\,U$ relative to the blades.

The solutions plotted in Figure 6 are a generalization of those presented in Reference [4], where a restrictive assumption of small swirl ($b \ll 1$) was made. It is important to notice that no information is obtained from the solution concerning the amplitude, shape, or wave length of the periodic solution $\tilde{h}(y)$. This is a result of the linearization of the problem, including the blade-characteristic curve. According to this result, *any* periodic function $\tilde{h}(y)$ supports itself by means of its own induced angles, provided only that $k + b$, $m\,\sigma$, k, and Δ satisfy equations (34).

Nonlinear Lift-Coefficient Curve [5]

In Reference [5], MARBLE attempted to avoid this situation by introducing a certain nonlinear lift-coefficient function in place of equations (23) and (25). This function, suggested by H. S. TSIEN, is

$$c_l[\alpha] = A\,\alpha - B\left(\alpha - C\,\frac{d\alpha}{dt}\right)^3, \tag{35}$$

where A, B, and C are constants and $d\alpha/dt$ denotes the time rate of change of α. He then assumed $\tilde{h}(y)$ to be a simple sine, and tried to find solutions of the rotating-stall problem in a manner analogous to what has been carried out above. Preliminary results were presented in Reference [5].

In general, the nonlinearity produces higher harmonics in the induced angle $\tilde{\alpha}$, even when $\tilde{h}(y)$ is sinusoidal; thus the problem of satisfying the homogeneous equations is a much more complicated one. In other words, a mathematical difficulty arises in the determination of the Fourier coefficients of $\tilde{h}(y)$, since they are not independent of one another. In this situation Professor MARBLE has concluded that it is more fruitful to use a different description of the nonlinear blade characteristic at stalling, which will be discussed below.

Blade-Characteristic Relations of Channel Type

In some other investigations of the same phenomenon, the concept of the blade row as a lattice of airfoils has been discarded. Instead, the row has been treated as an ensemble of channels.

Variable-Area Channels ([1] and [9])

In Reference [1], EMMONS suggested that the effect of partial stalling of the channel between two blades could be represented as a partial constriction of the passage area through the channel. He defined a flow coefficient $\varkappa$ for the passage such that

$$U + u_0 = \text{const} \cdot \varkappa . \tag{36}$$

This was based on the assumption that the static pressure behind the blade row would remain uniform in spite of the asymmetric flow pattern, so that the only variable affecting the flow through the row at any point would be the degreee of constriction, i.e., the degree of boundary-layer separation. EMMONS further assumed that the flow coefficient is determined by the inlet angle $\beta_i(y)$. For the purposes of his investigation he linearized the expression for this angle, viz.,

$$\tilde{\beta}_i = \frac{b + k}{1 + (b + k)^2} \left[\frac{v_-}{(b + k)\, U} - \frac{u_0}{U} \right] \tag{37}$$

and assumed a linear relationship between $\varkappa$ and β_i in steady flow. For unsteady flow, he assumed that $\varkappa$ increases at a rate proportional to its deviation from this steady-flow value, for any given $\tilde{\beta}_i$; this is equivalent to assuming a certain type of lag between $\tilde{\beta}_i$ and $\tilde{\varkappa}$. The result of these assumptions is to provide a blade-characteristic function in the form

$$u'_0(y) = K_1\, u_0 - K_2\, v_- , \tag{38}$$

where K_1 and K_2 are real constants involving the various constants of proportionality of EMMONS' theory as well as k and b.

According to this theory, it will be noted, the flow pattern upstream of the blade row is independent of the flow downstream. Equations (18) are not needed; the only unknowns are $u_0(y)$ and $v_-(y)$, and they are determined by equations (14) and (38). Assume that $u_0(y)$ is given as a Fourier series (real parts being implied, as before); then

$$u_0(y) = \sum_{n=1}^{\infty} u_n\, e^{2\pi i n y/l}, \tag{39}$$

$$v_-(y) = -\frac{1}{\pi} \int_{-\infty}^{\infty} \frac{u_0(\eta)\, d\eta}{y - \eta} = i \sum_{n=1}^{\infty} u_n\, e^{2\pi i n y/l} \tag{40}$$

$$u'_0(y) = \frac{2\pi i}{l} \sum_{n=1}^{\infty} n\, u_n\, e^{2\pi i n y/l}, \tag{41}$$

so that equation (38) requires

$$\frac{2\pi i}{l}\, n = K_1 - i\, K_2 . \tag{42}$$

EMMONS has already noted [1] that this means that $K_1 = 0$ for a flow pattern propagating without growing or subsiding. This amounts to a condition on the slope of the curve of $\varkappa$ versus β_i; it seems to be analogous to the condition on $m\,\sigma$ obtained in the earlier analysis [equation (34)]. He did not mention that it also requires a special relationship between n and K_2; i.e., his theory states that the rotating-stall pattern must be purely sinusoidal with a wave length determined by the constants of his blade-characteristic relations and parameters k and b. The nature of this relationship is such that the relative speed $k\,U$ decreases with increasing n, i.e., with decreasing wave length of the pattern, all other parameters being the same.

This theory has been extended by STENNING [9]. STENNING's analysis is basically the same as EMMONS', but an attempt is made, in introducing time lag, to distinguish between 'boundary-layer lag' and the time lag due to inertia of the fluid contained within any blade passage; it is concluded that the latter is more important. The same assumption of uniform downstream static pressure is made and is defended as an approximation for stall patterns whose wave length is not large compared to the circumferential blade spacing.

STENNING'S results are similar to EMMONS'. Again two relations are found for steadily rotating stall patterns, one of which is a condition on the slope of the curve of flow coefficient $\varkappa$. The other (which is fully discussed by STENNING) restricts the steady pattern to a pure sine curve and relates k, b, und l/n in such a way that sinusoidal patterns of long wave length rotate faster relative to the blades than those of shorter wave length, all other effects being the same. STENNING presents some experimental data, obtained by Professor EMMONS, which seem to support this conclusion regarding the effect of wave length on speed of propagation. There are other experimental data, however (e.g., in Reference [2]), which do not show the same tendency.

Channel Relations Used in Reference [7]

Besides the 'airfoil' analysis already discussed above, Reference [7] gives a solution based on 'channel' equations different from EMMONS' and STENNING'S. Following a suggestion of Professor RANNIE, the author undertook to set up blade-characteristic relations that would resemble the results of steady-flow cascade tests. Such results are sketched in Figure 7, where it is indicated that (1) stalling of a stationary cascade is indicated by a sudden increase of total-head loss, $-\Delta H$, plotted against inlet angle β_i, and (2) the outlet angle β_o is substantially constant, for high-solidity cascades, even in the stall. The first of these conclusions must be modified to apply to a moving cascade, of course. For this case the corresponding curve of ΔH versus β_i would have the character of Figure 7 (*c*).

These curves suggest the use of the following blade-characteristic relations:

$$\beta_o = \text{constant}, \quad \text{or} \quad \tilde{\beta}_o = 0 \tag{43}$$

and, linearizing the curve of Figure 7(*c*) at the appropriate uniform-turning

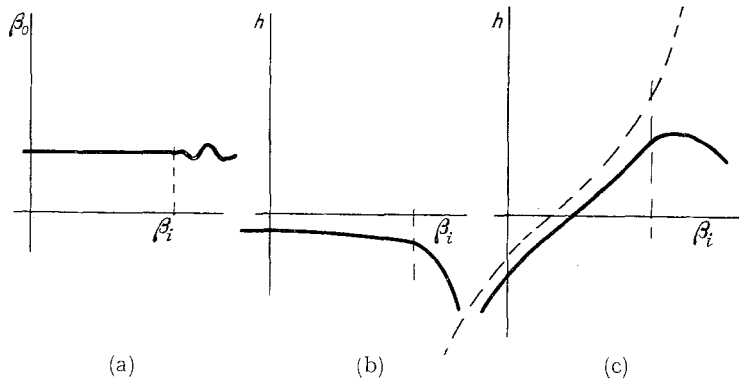

Figure 7

Sketches showing (*a*) outlet angle and (*b*) total-pressure rise of typical stationary cascades and (*c*) corresponding total-pressure rise for rotating cascades. β_i is the inlet angle.

values,

$$\tilde{h} = -M\,\tilde{\beta}_i \quad (M = \text{constant}) . \tag{44}$$

The sign convention adopted here is such that M is positive for the stalled blade row.

As a generalization of these relations, the type of time lag (phase lag) observed by MENDELSON for airfoils was introduced at this point in Reference [7]. This was, of course, rather arbitrary. It is justified only by analogy with the airfoil result. The process of viscous separation and energy loss described by the channel relations is similar to the process of airfoil stalling, which MENDELSON found to be approximated by a phase lag of this type. Furthermore, it seems to be the only type of lag that can be introduced without automatically restricting the flow pattern to a simple sine. Rather, the enormous generality of Fourier series is maintained; i.e., solutions will be found for which

$$\tilde{\beta}_i(y) = \sum_{n=1}^{\infty} \beta_n\, e^{2\pi i n y/l} \tag{45}$$

and

$$\tilde{h}(y) = -M \sum_{n=1}^{\infty} \beta_n\, e^{i[2\pi n (y/l)+\delta]}, \tag{46}$$

where δ is a real constant.

Again the process of solution begins by finding the Fourier coefficients β_n corresponding to the h_n of equation (26). The linearized expression for $\tilde{\beta}_o$ is the same as equation (37) but with $\tilde{\beta}_o$ written in place of $\tilde{\beta}_i$ and $\tilde{v}_+$ in place of v_-; thus the first channel relation, equation (43), states that $\tilde{v}_+ = (b + k)\, u_0$, and $\tilde{\beta}_i$, from equation (37), becomes

$$\tilde{\beta}_i(y) = \frac{1}{1 + (b + k)^2} \cdot \frac{v_- - \tilde{v}_+}{U} . \tag{47}$$

Now, an expression for $v_- - \tilde{v}_+$, involving u_0, is obtained from equations (14) and (18):

$$v_-(y) - \tilde{v}_+(y) = -\frac{2}{\pi} \int_{-\infty}^{\infty} \frac{u_0(\eta)\, d\eta}{y - \eta} - \frac{b}{1 + b^2}\, U \tilde{h}(y) + \frac{1}{\pi} \cdot \frac{U}{1 + b^2} \int_{-\infty}^{\infty} \frac{\tilde{h}(\eta)\, d\eta}{y - \eta} . \tag{48}$$

Another expression for the same quantity follows from equation (14) and (43):

$$v_-(y) - \tilde{v}_+(y) = -\frac{1}{\pi} \int_{-\infty}^{\infty} \frac{u_0(\eta)\, d\eta}{y - \eta} - (b + k)\, u_0(y) . \tag{49}$$

One can obviously eliminate $v_- - \tilde{v}_+$ from these two equations, obtaining

$$\frac{1}{\pi} \int_{-\infty}^{\infty} \frac{u_0(\eta)\, d\eta}{y - \eta} - (b + k)\, u_0(y) = \frac{U}{1 + b^2} \left\{ - b\, \tilde{h}(y) + \frac{1}{\pi} \int_{-\infty}^{\infty} \frac{\tilde{h}(\eta)\, d\eta}{y - \eta} \right\} . \tag{50}$$

If u_n denote the Fourier coefficients of $u_0(y)$, so that

$$u_0(y) = \sum u_n\, e^{2\pi i n y/l} ,$$

equation (50) relates u_n to h_n:

$$u_n = \frac{U}{1 + b^2} \cdot \frac{i + b}{i + b + k}\, h_n . \tag{51}$$

Now, making use of equation (49) again, one has a simple relation between u_n and the Fourier coefficients of $v_- - \tilde{v}_+$, which in turn are related to β_n in equation (47). Finally, from equation (46) the homogeneous equation of the problem becomes

$$\left.\begin{aligned} \sum_{n=1}^{\infty} h_n\, e^{2\pi i n y/l} &= -M \frac{1}{1 + (b + k)^2} \cdot \frac{1}{U} \left[i - (b + k) \right] \sum_{n=1}^{\infty} u_n\, e^{i\left[2\pi n (y/l) + \delta\right]} \\ &= -M \frac{1}{1 + (b + k)^2} \cdot \frac{i - (b + k)}{i + b + k} \cdot \frac{i + b}{1 + b^2} \sum_{n=1}^{\infty} h_n\, e^{i\left[2\pi n (y/l) + \delta\right]} . \end{aligned}\right\} \tag{52}$$

This requires both

$$\frac{M}{\sqrt{1+b^2}} = 1 + (b+k)^2 \tag{53}$$

and

$$\tan\delta = \frac{1+b^2-k^2}{b\,(b+k)^2+2k+b}\,. \tag{54}$$

When equations (53) and (54) are both satisfied, any periodic flow pattern is in equilibrium and rotates steadily. The compatible values of M, k, and $b+k$

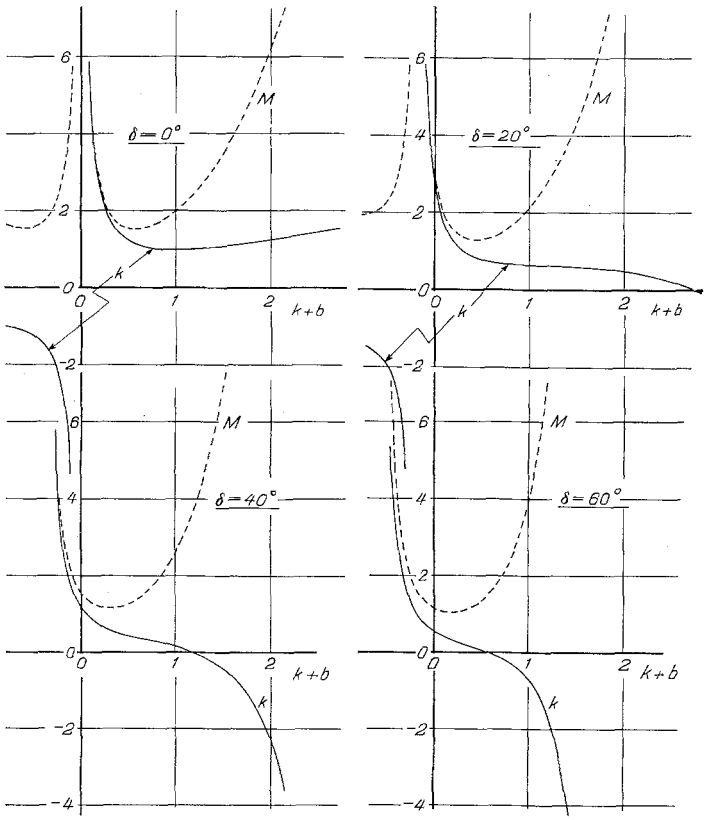

Figure 8

Rotating-stall solutions based on blade-characteristic relations of channel type. The abscissa, $k+b$, is the tangent of the mean inlet angle β_i.

are plotted in Figure 8 for several values of the phase-lag angle δ. Again the independent variable is $b+k$, the tangent of the mean (undisturbed) angle of inflow relative to the blades, $\tan\beta_i$. All the interesting values of M are positive,

which means that the blade row must be so fully stalled as to have a negative characteristic slope, as defined in Figure 7(*c*). Then rotating stall can occur at a certain relative speed k, with or without lag.

Marble's Discontinuous Blade Characteristic

In Reference [8], Professor MARBLE has employed a nonlinear blade characteristic of a most interesting type, namely, a relation exhibiting a discontinuity at the stall. That such characteristics should be used was suggested in Reference [4] but was not carried out. MARBLE's first blade-characteristic relation is a generalization of equation (43); viz.,

$$\tilde{\beta}_0 = \text{const} \cdot \tilde{\beta}_i \,. \tag{55}$$

His second relation is expressed in terms of the static-pressure rise across the blade row,

$$\Delta p \equiv p(+\,0, y) - p(-\,0, y) \,.$$

It is his assumption that this pressure rise varies approximately linearly with the inlet angle β_i below the stall but drops to zero when stalling occurs. This relation is sketched in Figure 9.

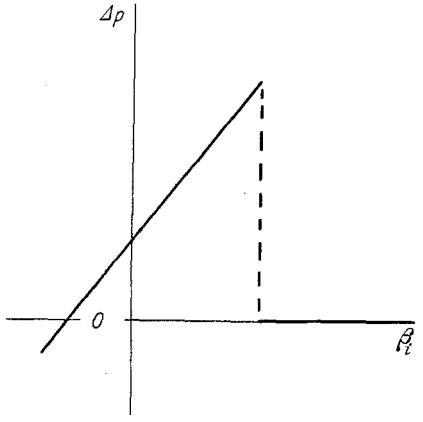

Figure 9

Sketch showing MARBLE's discontinuous blade-characteristic function [8]. Δp denotes static-pressure rise and β_i the inlet angle.

For convenience in applying this condition, MARBLE works with the dependent variable $p(x, y)$ instead of the velocity components used in the previous investigations. Since the small-perturbation approximation is employed, the pressure perturbation satisfies LAPLACE's equation both upstream and downstream of the blade row. MARBLE shows that the angles $\tilde{\beta}_i$ and $\tilde{\beta}_o$ can also be

expressed quite simply in terms of the pressure perturbation and its harmonic conjugate. Thus, the boundary-value problem of the two-dimensional blade row is reduced to finding a harmonic function whose real and imaginary parts, along the axis $x = 0$, satisfy certain relations derived from equation (55) and the characteristic sketched in Figure 9.

The results of this analysis will not be reproduced here. They consist of the propagation speed ratio k and the *percentage of circumference stalled*, both as functions of $k + b$, the tangent of the mean inlet angle. MARBLE finds that k is insensitive to variations of $k + b$ for values of $k + b$ near 1, which is a typical value for axial-flow compressors. It is interesting to notice that in one particular case that he studies in detail, in which the constant of equation (55) is taken equal to zero, so that this relation coincides with equation (43) of the earlier, SEARS analysis, his curve of k versus $k + b$ is identical with the one plotted in Figure 8 for $\delta = 0$. Presumably the effects of lag could be introduced into MARBLE's analysis, but this has not been done.

The most interesting result in MARBLE's work is the percentage of circumference stalled, or the ratio of stalled to unstalled length in the periodic flow pattern. This increases rapidly from 0 to 1·0 as $k + b$ is increased above the value where partial stalling first appears. The slope of this increase depends on the magnitude of the pressure rise Δp across the unstalled portions but seems to be relatively insensitive to the slope of the unstalled portion of the blade characteristic.

Comparison with Experiment

Practically the only comparison that can be made with experimental results at present is the comparison of measured and predicted rates of stall propagation. Such a comparison is attempted in Figure 10, where the curves of k versus $k + b$ are collected from Figures 6 and 8. The experimental points in this figure are taken from the report of IURA and RANNIE [2]. They represent the conditions of the rotor and stator rows of their experimental compressor at the onset of rotating stall. It is not known whether the rotor or stator rows were responsible for the stalling. To be more precise, it must be admitted that the present single-row theories are only roughly applicable to IURA's and RANNIE's three-stage machine, and the attempted comparison is based on the assumptions (1) that either stator *or* rotor rows (but not both) must be responsible for the onset of rotating stall and (2) that the presence of other rows does not seriously affect the results, as compared to those of the idealized single-row model.

The dashed lines emanating from the experimental points in Figure 10 show the approximate variation of k with $k + b$, for rotors and stators, respectively, for flow quantities smaller than that at which rotating stall commences.

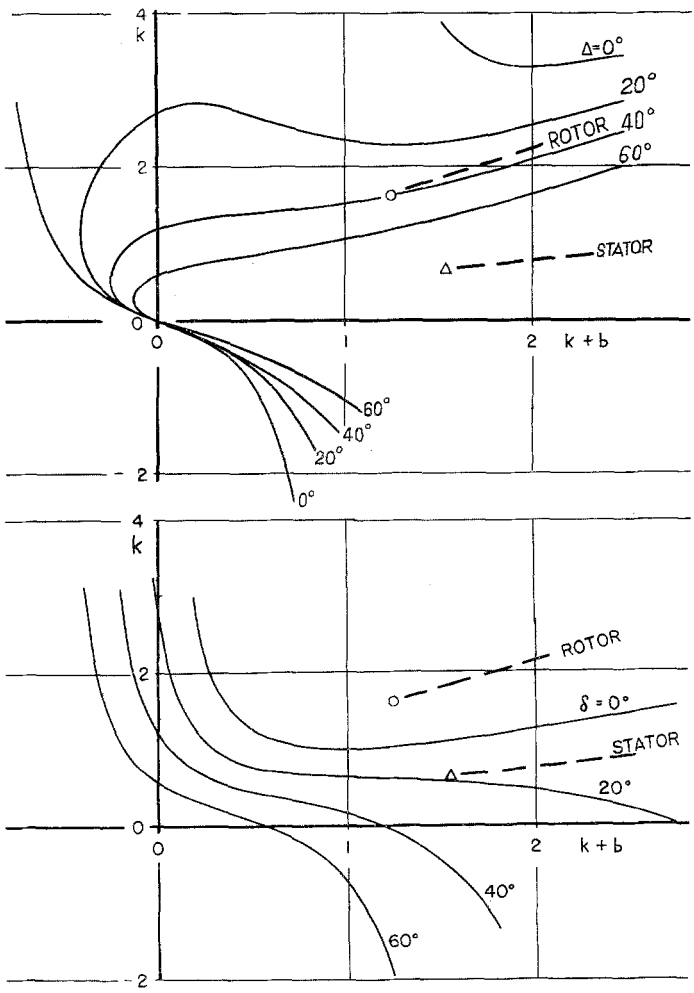

Figure 10

Comparison of measured rates of stall rotation [2] with theoretical values based on airfoil (above) and channel (below) types of blade characteristics, from Figures 6 and 8. The abscissa, $k + b$, is the tangent of the mean inlet angle $\bar{\beta}_i$. The experimental points and dashed lines are from Reference [2], computed for rotors and stators, respectively.

It is seen that the experimental points fall within the range of the theoretical diagrams based on either 'airfoil' or 'channel'-type blade characteristics. However, the point denoting rotor conditions requires either negative lag or excessive positive lag if the 'channel' theory is adopted, while the point denoting stator conditions requires a rather large value of the lag (compared

to MENDELSON'S observations) in the 'airfoil' theory. There is an interesting coincidence between the experimental curve for rotor conditions (the upper dashed line) and the theoretical curve for constant phase lag Δ in Figure 10*a*. Nevertheless, it is clear that the available comparison with experimental results does not lead to any general conclusions.

Discussion and Conclusions

In this paper, several attempts to explain theoretically the phenomenon of rotating stall have been described. These are all based on the assumptions of a single row of closely spaced blades and the small perturbation type of flow. They are, therefore, probably inadequate to describe the conditions observed in multistage axial compressors. On the other hand, they provide at least a qualitative explanation of the phenomenon, and they are in agreement in their conclusion that steadily rotating patterns may occur in stalled, rigid blade rows.

In addition to the limitations imposed by their simplifying assumptions, these theories all have the drawback that they involve several unknown parameters. In the analysis based on 'airfoil' relations, for example, both the lift-curve slope m and the lag angle Δ are involved. Unfortunately, one's understanding of stalled-airfoil flow is insufficient to determine either of these quantities with assurance. Each of the analyses discussed has this drawback, although the governing parameters are expressed in other terms. It appears that more definitive theoretical and experimental work on stalled airfoils and (or) channels is needed.

Presumably, the several different analyses, being alike in basic structure but differing in the assumed blade-characteristic relations, have relative advantages and disadvantages, but it is difficult to choose between them on the basis of the available experimental data. The present author believes that there is a considerable virtue in the assumption of MENDELSON'S type of lag, i.e., phase lag independent of frequency, since this avoids the limitation of flow patterns to purely sinusoidal ones. This limitation has occurred, probably unintentionally, in the work of EMMONS [1] and STENNING [9]. Undoubtedly MARBLE'S use of a discontinuous characteristic [8] provides information unavailable in the linearized treatments. It seems questionable whether the blade-characteristic function of Figure 9 is realistic, however, for the static-pressure rise through a blade row surely does not vanish when stalling occurs. In this connection, the contrast between MARBLE'S assumptions and those of EMMONS and STENNING is striking: the former assumes a violent reduction of static pressure downstream of the stalled portions of the blade row, while the latter assume that the same quantity is uniformly distributed. It should not be difficult to make a choice between these two assumptions on the basis of suitable future experimental observations.

Addendum Supplied October 1955

Since the manuscript of the present paper was submitted for publication, additional investigations of rotating stall, including interesting experimental results, have appeared (References [12], [13], [14], [15], [16]). The newer experimental results (References [13] and [16]) are particularly pertinent to any assessment of the theories, because they have been obtained in single-row configurations, which more closely resemble the theoretical models. Also, since static-pressure fluctuations were measured before and behind the rotors in these tests, these results cast considerable light on the assumptions made by MARBLE and STENNING in their theories.

The agreement between measured rates of stall propagation and those predicted by the theories of Reference [7] is similar to that shown here in Figure 10. (The present author does not agree with the way this comparison was carried out in Reference [16] and has made his own comparison, to which the preceding statement applies.) Fortunately, the question of whether rotor or stator was stalled, which complicated the matter in Figure 10, does not occur in these single-row comparisons. The authors of Reference [13] conclude, in part: 'The measured stall-propagation rates can be made to agree with theoretical predictions by adjusting certain theoretically undetermined factors appearing in the theories.'

REFERENCES

[1] EMMONS, H. W., PEARSON, C. E., and GRANT, H. P., *Compressor Surge and Stall Propagation*, Trans. A. S. M. E., *77*, 455–467 (1955).

[2] IURA, T., and RANNIE, W. D., *Observations of Propagating Stall in Axial-Flow Compressors*, Trans. A. S. M. E., *76*, 463–471 (1954).

[3] HUPPERT, MERLE C., and BENSER, WILLIAM A., *Some Stall and Surge Phenomena in Axial-Flow Compressors*, J. aeron. Sci. *20*, 835–845 (1953).

[4] SEARS, W. R., *On Asymmetric Flow in an Axial-Flow Compressor Stage*, J. appl. Mech. *20*, 57–62 (1953).

[5] MARBLE, FRANK E., *Propagation of Stall in Compressor Blade Rows*, Presented at 21st Annual Meeting, Inst. aeron. Sci., New York, January 26, 1953.

[6] MENDELSON, ALEXANDER, *Effect of Aerodynamic Hysteresis on Critical Flutter Speed at Stall*, J. aeron. Sci. *16*, 645–652 (1949).

[7] SEARS, W. R., *A Theory of 'Rotating Stall' in Axial-Flow Compressors*, Grad. School aeron. Eng., Cornell Univ., Ithaca, N.Y., January 1, 1953. Prepared under Contract AF 33 (038)–21406, U.S. Air Force, Office Sci. Res., R. and D. Command, Baltimore, Md.

[8] MARBLE, FRANK E., *Propagation of Stall in a Compressor Blade Row*, J. aeron. Sci. *22*, 541–554 (1955).

[9] STENNING, ALAN H., *Stall Propagation in a Cascade of Airfoils*, Gas Turbine Lab., Mass. Inst. Tech., Cambridge, Mass., Rep. No. 25, May, 1954. Prepared under Contract NAw-6303, Nat. Advis. Comm. Aeron., Washington, D.C.

[10] LAMB, H., *Hydrodynamics*, 6th edition (Cambridge University Press, London 1932), pp. 243–244.
[11] SEARS, W. R., *A New Treatment of the Lifting-Line Wing Theory, with Applications to Rigid and Elastic Wings*, Quart. appl. Math. *6*, 239–255 (1948). See especially pp. 243–244.
[12] SMITH, A. G., and FLETCHER, P. J., *Observations on the Surging of Various Low-Speed Fans and Compressors*, Nat. Gas Turbine Estab. Memo. No. M. 219 (July 1954).
[13] COSTILLOW, ELEANOR L., and HUPPERT, MERLE C., *Rotating-Stall Characteristics of a Rotor with High Hub-Tip Radius Ratio*, Nat. Advis. Comm. Aeron. Techn. Note No. 3518 (1955).
[14] STENNING, ALAN H., *Stall Propagation in Cascades of Airfoils*, J. aeron. Sci. *21*, 711–713 (1954).
[15] STENNING, A. H., *Stall Propagation in Axial Compressors*, Gas Turbine Lab., Mass. Inst. Techn., Cambridge, Mass., Rep. No. 28 (April 1955). Prepared under Contract NAw-6375, Nat. Advis. Comm. Aeron., Washington, D. C.
[16] MONTGOMERY, STEPHEN R., and BRAUN, LT. JOSEPH J., *An Investigation of Rotating Stall in a Single Stage Axial Compressor*, Gas Turbine Lab., Mass. Inst. Techn., Cambridge, Mass., Rep. No. 29 (May 1955). Prepared under Contract NAw-6375, Nat. Advis. Comm. Aeron., Washington, D. C.

Abstract

The phenomenon known as 'rotating stall' is described. Basically, it involves a nonuniform pattern of flow, steadily rotating relative to both the fixed and the rotating blades of axial-flow compressors. Attempts to analyze the phenomenon by means of small-perturbation theories are reviewed. It is shown that the work of several investigators can be included in a single formulation and that they differ only in the type of blade-characteristic relations assumed. The present author's analyses based on linearized 'airfoil' and 'channel' relations are presented in detail. The various theories coincide in the qualitative conclusion that self-induced rotating-stall patterns can occur in stalled, rigid blade rows. A comparison with available experimental results is inconclusive, so far as a choice between the several theories is concerned.

Zusammenfassung

Die als «umlaufende Abreißströmung» bekannte Erscheinung wird beschrieben, welche durch ein Strömungsbild gekennzeichnet ist, das sowohl bezüglich des Stators wie auch des Rotors in einem axialen Verdichter stetig umläuft. Eine Übersicht der theoretischen Ansätze zur Beschreibung dieser Erscheinung im Rahmen einer Störungsrechnung ist gegeben. Es kann gezeigt werden, dass die meisten Ansätze einheitlich behandelt werden können und sich nur in der angenommenen Schaufelcharakteristik unterscheiden. Berechnungen des Verfassers auf Grund von linearisierten «Auftriebskurven» und «Kanalbeziehungen» sind ausführlich dargestellt. Alle Theorien liefern das gleiche qualitative Ergebnis eines selbstinduzierten, umlaufenden Strömungsbildes in einem starren Gitter mit abgerissener Strömung. Ein Vergleich mit Versuchen ergibt vorläufig keine zwingenden Schlüsse betreffend die beste Wahl zwischen den Theorien.

(Received: August 30, 1954.)